

A plot of current-voltage trajectories against non-controlled FCS polarization curves is shown in Figure 15. Immediately after a step change in current, the voltage drops along the fixed cathode pressure polarization curve based on the high frequency impedance  $R_{\text{cFCS}}^{\text{high}} = 0.3 \Omega$ . After the initial transient, the controlled FCS shows a voltage that transitions to another polarization curve of higher cathode pressure. This behavior is the reason for smaller cFCS resistance  $R_{\text{cFCS}}^{\text{low}} = 0.05 \Omega$  at low frequencies. The increase in operating cathode pressure is dictated by the  $\lambda_{\text{O}_2}$  regulation. This phenomenon is associated with the high pressure air supply through a high speed compressor. A low pressure FCS will have similar controlled and uncontrolled impedances, primarily due to the approximately constant operating pressure.

## Tradeoff Between Two Performance Objectives

When there is no additional energy storage device, such as a battery or ultra-capacitor, the power used to run the compressor motor needs to be taken from the FC stack. A transient step change in stack current requires rapid increase in air flow to prevent depletion of cathode oxygen. The rapid air flow increase, consequently, requires a large amount of power drawn by the compressor motor ( $P_{\text{cm}}$ ) and thus increases parasitic loss, which affects the system net power  $P_{\text{net}} = P_{\text{FC}} - P_{\text{cm}}$ .

The control problem we have considered so far is the single-input, single-output (SISO) problem of controlling the compressor voltage  $u = v_{\text{cm}}$  to regulate the oxygen excess ratio  $z_2 = \lambda_{\text{O}_2}$ . Achieving the desired value of  $z_2 = \lambda_{\text{O}_2}$  during steady-state ensures that the desired net power  $z_1 = P_{\text{net}}$  is obtained. During transient, however, the two objectives are independent, resulting in the single-input two-output (SITO) control problem [22] shown in Figure 16.

Let us first consider the effects of the exogenous input  $I_{\text{st}}$  and the control signal  $v_{\text{cm}}$  on the first performance variable  $z_1 = P_{\text{net}}(I_{\text{st}}, v_{\text{cm}}) = P_{\text{FC}}(I_{\text{st}}, v_{\text{cm}}) - P_{\text{cm}}(v_{\text{cm}})$ , or, in the linear sense,  $\delta z_1 = G_{z_1 w} \delta w + G_{z_1 u} \delta u$ . As can be seen from the step responses in Figure 17,  $I_{\text{st}}$  has a positive effect on the net power. On the other hand, the compressor voltage  $v_{\text{cm}}$  causes an initial inverse response in the net power due to a nonminimum phase zero. The last plot in Figure 17 shows the net power during a step change in  $I_{\text{st}}$ , together with a step change in  $v_{\text{cm}}$ , which in steady-state ensures that  $z_2 = \lambda_{\text{O}_2}^d = 2$ . It can be seen that the time needed for  $P_{\text{net}}$  to reach the desired value is approximately one second.

It is apparent that to speed up the  $P_{\text{net}}$  response, we need either a larger magnitude of  $I_{\text{st}}$  to increase stack power or smaller value of  $v_{\text{cm}}$  to decrease the parasitic losses. Both cases degrade the speed of  $\lambda_{\text{O}_2}$  response, because larger  $I_{\text{st}}$  causes additional drops in  $\lambda_{\text{O}_2}$ , while smaller  $v_{\text{cm}}$  slows down the recovery rate of  $\lambda_{\text{O}_2}$ . The

tradeoff between  $P_{\text{net}}$  and  $\lambda_{\text{O}_2}$  responses always exists because there is only one control actuator. The actuator must compromise between the two conflicting performance variables.

We systematically explore the tradeoff by setting up the LQ control problem with the cost function

$$J = \int_0^\infty Q_{z_1} z_1^2 + Q_{z_2} z_2^2 + Ru^2 + Q_I q^2 dt. \quad (46)$$

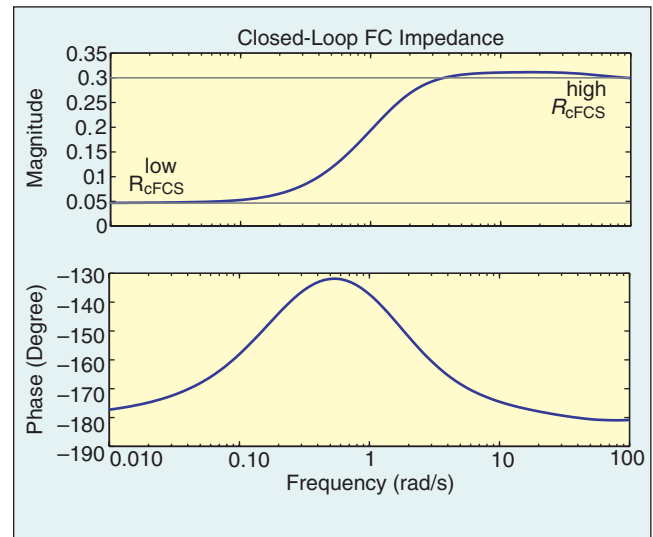


**Figure 14.** Impedance of the controlled FC stack. Current signals with frequencies smaller than 0.1 rad/s cause six times lower impedance than currents with frequencies larger than 10 rad/s.

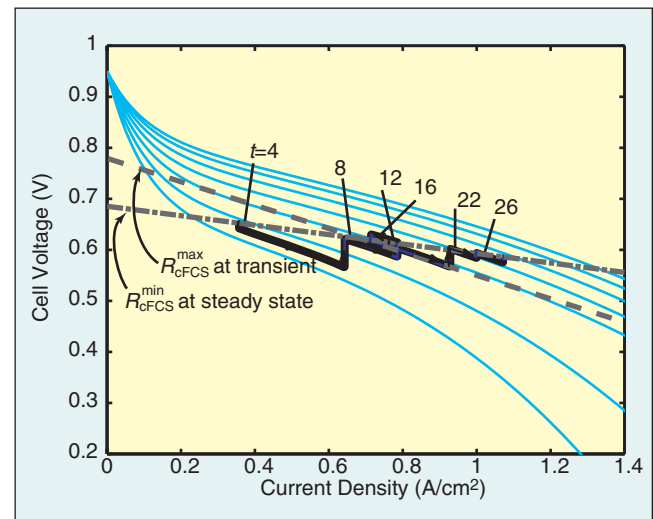


**Figure 15.** Current-voltage trajectories in nonlinear simulation. These trajectories correspond to the nonlinear simulation of Figure 7.